

## Nonlocality and many-body effects in the optical properties of semiconductors

B. Adolph, V. I. Gavrilenko, K. Tenelsen, and F. Bechstedt

*Friedrich-Schiller-Universität, Institut für Festkörpertheorie und Theoretische Optik, Max-Wien-Platz 1, 07743 Jena, Germany*

R. Del Sole

*Dipartimento di Fisica, Università di Roma "Tor Vergata," via del Ricerca Scientifica, I-00133 Roma, Italy*

(Received 1 September 1995; revised manuscript received 14 November 1995)

We report numerical calculations of the frequency-dependent dielectric function for different gauges of the electromagnetic field in the optical transition operator. Comparing the results, we draw conclusions about the importance of different nonlocality effects entering the calculations. Apart from the spatial inhomogeneity related to the atomic structure of matter, they are due to nonlocal pseudopotentials, quasiparticle self-energies, and the incompleteness of the basis functions. Besides their influence on optical spectra, their effect on the validity of the  $f$ -sum rule and the magnitude of the resulting dielectric constants is also discussed. We present results for optical spectra where the many-body quasiparticle effect is included beyond the scissors-operator approximation. The group-IV materials Si, SiC, and C are considered as model substances.

### I. INTRODUCTION

In the past few years, a number of highly accurate calculations of optical and dielectric properties of semiconductors have appeared.<sup>1-10</sup> In general, they are based on the independent-particle approximation<sup>11-13</sup> [often called the random-phase approximation (RPA)] and a first-principles description of the electronic and atomic structure in the framework of the density-functional theory (DFT) (Ref. 14) in the local-density approximation (LDA).<sup>15</sup> These papers supplement earlier work in the field<sup>16-20</sup> (and references therein), in which in addition local-field effects and excitonic effects have been partially included.

The most serious error of band-structure calculations within the DFT-LDA for semiconductors and insulators concerns the discrepancies between the Kohn-Sham eigenvalues<sup>15</sup> and experimental band energies.<sup>20,21</sup> The problem of the underestimation of the gaps between filled and empty states has been solved by taking into account quasiparticle (QP) corrections<sup>22,23</sup> within the  $GW$  approximation<sup>24,25</sup> for the many-body exchange-correlation (XC) self-energy for electrons and holes, which is, in general, nonlocal in space and time. The inclusion of QP corrections allows agreement of theory with one-electron energies obtained from direct and inverse photoemission experiments at a level of about 0.1 eV, when the bands of the underlying DFT-LDA band structure already possess the correct energetical ordering, but certain underestimated gaps. In these cases, the QP wave functions are in excellent agreement (wave-function overlaps exceeding 0.999) with the DFT-LDA ones, at least for near gap excitations.<sup>22</sup> The simplest description of such QP corrections is the application of a scissors operator,<sup>26</sup> which displaces the empty and occupied band against each other by a rigid shift. In a series of papers, Levine and Allan<sup>5,10</sup> have shown how to calculate optical and dielectric properties within the QP scissors-operator approximation. However, this approach introduces two other difficulties: The oscillator-strength sum rule and the gauge invariance of the electromagnetic-field description are violated (the latter dif-

ficulty actually arises when the formulas defining the dielectric function are used naively).<sup>5,27</sup>

The most recent DFT-LDA calculations of the electronic structures are performed in the framework of the plane-wave pseudopotential method, where the Bloch functions of the valence and conduction electrons are expanded in terms of plane waves up to a certain energy cutoff and the electron-ion interaction is described by semilocal pseudopotentials of Bachelet-Hamann-Schlüter (BHS) type<sup>28</sup> or full nonlocal pseudopotentials of Kleinman-Bylander (KB) type<sup>29</sup> or pseudopotentials generated by similar schemes. In any case, the effective potential in the single-particle Kohn-Sham equations<sup>15</sup> contains a spatially nonlocal contribution that requires a careful treatment of the optical transition operators in the different gauges.<sup>27,30,31</sup> A third type of nonlocality is due to numerical uncertainties related to the restriction of the wave-function basis in all explicit calculations. On the one hand, the number of plane waves is limited by the cutoff. On the other hand, only a finite number of conduction bands and wave vectors in the Brillouin zone are taken into account, which violates the closure relation of the Bloch functions. A fourth type of nonlocalities is due to the atomic structure of matter. These so-called local-field effects<sup>17,18</sup> are, therefore, always present in the calculation independent of the actual description of the electronic structure.

In the present paper, the introduced nonlocality and many-body effects (with the exception of local-field effects) are studied in more detail for the optical properties of semiconductors. As model substances the group-IV materials diamond (C), silicon (Si), and silicon carbide (SiC) crystallizing in diamond or zinc-blende structure are considered. We calculate joint density of states, the imaginary as well as real part of the frequency-dependent dielectric function, and the optical reflectivity. These studies are performed in the framework of two different gauges of the external electromagnetic field. Simultaneously, also the validity of the equivalence of longitudinal and transverse dielectric function, as well as the  $f$ -sum rule, is investigated analytically and numerically. All calculations are done starting from the independent-particle

approximation or independent-quasiparticle approximation, but varying the approximations and numerical details of the electronic-structure description.

Section II is devoted to the introduction of the longitudinal and transverse dielectric functions. The gauge invariance, as well as the oscillator-strength sum rule, are examined. Explicit formulas are derived. In Sec. III, we illustrate our analytical findings by computing the optical properties for C, Si, and SiC in different approximations and using different numerical limitations. In this section, we also present the first QP calculation of optical spectra beyond the scissors-operator approximation, by taking into account the full wave-vector and band-index dependence of the QP corrections. The most converged results are compared with experimental spectra. A brief summary and final remarks are given in Sec. IV.

## II. BASIS THEORY

### A. Dielectric function

In the independent-particle approximation and applying the RPA decoupling of the two-particle Green function, one obtains for the dielectric matrix,<sup>11–13,32</sup>

$$\varepsilon(\mathbf{q}+\mathbf{G}, \mathbf{q}+\mathbf{G}', \omega) = \delta_{\mathbf{G}\mathbf{G}'} - v(\mathbf{q}+\mathbf{G})P(\mathbf{q}+\mathbf{G}, \mathbf{q}+\mathbf{G}', \omega), \quad (1)$$

with  $v(\mathbf{q}+\mathbf{G}) = 4\pi e^2/|\mathbf{q}+\mathbf{G}|^2$  and the polarization function of independent particles  $P \equiv P_0$  ( $\eta \rightarrow +0$ ),

$$\begin{aligned} P_0(\mathbf{q}+\mathbf{G}, \mathbf{q}+\mathbf{G}', \omega) &= \frac{2}{V} \sum_{\mathbf{k}, \mathbf{k}'} \sum_{n, n'} \langle n\mathbf{k} | e^{i(\mathbf{q}+\mathbf{G}')\cdot\mathbf{x}'} | n'\mathbf{k}' \rangle \\ &\quad \times \langle n'\mathbf{k}' | e^{-i(\mathbf{q}+\mathbf{G})\cdot\mathbf{x}} | n\mathbf{k} \rangle \\ &\quad \times \frac{f(\varepsilon_{n'}(\mathbf{k}')) - f(\varepsilon_n(\mathbf{k}))}{\varepsilon_{n'}(\mathbf{k}') - \varepsilon_n(\mathbf{k}) + \hbar(\omega + i\eta)}. \end{aligned} \quad (2)$$

Here, Bloch integrals of exponential functions with the Bloch eigenfunctions  $|n\mathbf{k}\rangle$  belonging to the band index  $n$ , the wave vector  $\mathbf{k}$  in the first Brillouin zone (BZ), and the energy  $\varepsilon_n(\mathbf{k})$  are introduced. The Fermi functions  $f(\varepsilon)$  define the occupation of the bands. In the following, the Bloch states will be taken to have occupancies of 0 (conduction bands  $n=c$ ) or 1 (valence bands  $n=v$ ). The wave vector  $\mathbf{q}$  is also restricted to the first BZ, whereas the vectors  $\mathbf{G}, \mathbf{G}'$  are elements of the reciprocal Bravais lattice of the crystal with the volume  $V$ . Equations (1) and (2) represent the linear response (the charge density at wave vector  $\mathbf{q}+\mathbf{G}$  and at frequency  $\omega$ ) of a system of independent particles to a longitudinal microscopic perturbation (a scalar potential of wave vector  $\mathbf{q}+\mathbf{G}'$  and frequency  $\omega$ ). The restriction to a longitudinal perturbation that may be described by a scalar potential of the electromagnetic field alone is sufficient for the derivation of the density response.<sup>33,34</sup>

The RPA decoupling leading to Eq. (2) for the polarization function omits XC effects. On the other hand, we will describe the Bloch states by the solutions of the single-particle Kohn-Sham equations of the DFT-LDA; the bare Kohn-Sham eigenvalues are used within the independent-particle approximation, while QP corrections are added to

them within the independent-QP approximation. In both cases, we take into account some kind of XC effects. The corresponding formal generalization of the polarization function is  $P = P_0[1 - P_0 K_{XC}]^{-1}$ ,<sup>2,6,34</sup> where the kernel  $K_{XC}$  describes the XC effects taken into the two-particle Green function. Within the DFT, it may be represented by  $K_{XC} = \delta^2 E_{XC} / \delta n \delta n'$  with the electron density  $n$  and the total XC energy  $E_{XC}$ . The same result follows within the so-called time-dependent local-density approximation.<sup>5,35</sup> Within the DFT-LDA or the theory improved by QP corrections, it would be consistent to take  $K_{XC}$  into account. However, its LDA description gives rise to an incorrect behavior, at least for the most important diagonal Fourier components  $\mathbf{G} = \mathbf{G}'$ .<sup>2</sup> On the other hand, forms of the diagonal  $K_{XC}$ , which exhibit the correct asymptotic behavior and are almost derived in electron-gas theories,<sup>32,34,36</sup> bring the product  $P_0 K_{XC}$  to vanish for small wave vectors. This limit is, however, relevant for the description of optical properties. We, therefore, neglect corrections related to  $K_{XC}$  and restrict ourselves to expression (2) for the polarization function.

Since the local-field effects, however, do not change the peak position in the spectra very much, at least in the absorption spectra, but mostly the intensity distribution,<sup>17,32</sup> we neglect them in the following. From Eqs. (1) and (2), one obtains for the corresponding longitudinal dielectric function with  $\mathbf{G} = \mathbf{G}' = 0$  and  $\mathbf{q} \rightarrow 0$ ,

$$\begin{aligned} \varepsilon_l(\mathbf{q}, \omega) &= \lim_{\mathbf{q} \rightarrow 0} \left\{ 1 + v(\mathbf{q}) \frac{4}{V} \right. \\ &\quad \left. \times \sum_{\mathbf{k}, \mathbf{k}'} \sum_{c, v} \frac{[\varepsilon_c(\mathbf{k}) - \varepsilon_v(\mathbf{k}')][\langle c\mathbf{k} | e^{i\mathbf{q}\mathbf{x}} | v\mathbf{k}' \rangle]^2}{[\varepsilon_c(\mathbf{k}) - \varepsilon_v(\mathbf{k}')]^2 - \hbar^2(\omega + i\eta)^2} \right\}. \end{aligned} \quad (3)$$

### B. Gauge invariance

The dielectric function may be also derived within the transverse-response formalism, where the light-matter interaction is described by the coupling of the vector potential with the current density of the electrons, i.e., the so-called Coulomb<sup>33</sup> or velocity<sup>27,30</sup> gauge. In this gauge, the polarization function is related to the current-current correlation function.<sup>34</sup> To derive only the longitudinal part of the dielectric function, we go another way and transform expression (3). The limit of vanishing photon wave vectors can be easily performed in Eq. (3). However, this has to be done with care. Otherwise, ill-defined quantities as matrix elements of the dipole operator appear. A better way is to use the relation

$$\langle c\mathbf{k} | [e^{i\mathbf{q}\mathbf{x}}, H]_- | v\mathbf{k}' \rangle = [\varepsilon_v(\mathbf{k}') - \varepsilon_c(\mathbf{k})] \langle c\mathbf{k} | e^{i\mathbf{q}\mathbf{x}} | v\mathbf{k}' \rangle, \quad (4)$$

where  $H$  denotes the single-particle Hamiltonian fulfilling the Kohn-Sham equations  $H|n\mathbf{k}\rangle = \varepsilon_n(\mathbf{k})|n\mathbf{k}\rangle$  for both local and nonlocal potentials.<sup>37</sup> Using Eq. (4) and the fact that the two involved bands are different, the result of the limit  $\mathbf{q} \rightarrow 0$  can be related to matrix elements of the velocity operator  $v_\alpha$  in a certain Cartesian direction  $\alpha$ ,

$$v_\alpha = \frac{i}{\hbar} [H, x_\alpha]_- . \quad (5)$$

From Eq. (3), one obtains

$$\varepsilon_l(\mathbf{q}, \omega) = \sum_{\alpha\beta=x,y,z} \frac{q_\alpha q_\beta}{q^2} \varepsilon_{\alpha\beta}(\omega), \quad (6)$$

with

$$\begin{aligned} \varepsilon_{\alpha\beta}(\omega) &= \delta_{\alpha\beta} + \frac{16\pi e^2 \hbar^2}{V} \sum_{\mathbf{k}} \sum_{c,v} \frac{1}{[\varepsilon_c(\mathbf{k}) - \varepsilon_v(\mathbf{k})]} \\ &\times \frac{\langle c\mathbf{k}|v_\alpha|v\mathbf{k}\rangle \langle v\mathbf{k}|v_\beta|c\mathbf{k}\rangle}{[\varepsilon_c(\mathbf{k}) - \varepsilon_v(\mathbf{k})]^2 - \hbar^2(\omega + i\eta)^2}. \end{aligned} \quad (7)$$

When the Cartesian coordinate system is defined by the principal axes of the crystal, the dielectric tensor is diagonal. The diagonal elements  $\varepsilon_{\alpha\alpha}(\omega)$  of the dielectric tensor can be calculated in two different ways. It can be directly evaluated from Eq. (3) in the  $\mathbf{q} \rightarrow 0$  limit for suitable choices of the wave-vector direction parallel to the principal axes of the tensor. The second possibility starts from expression (7). One advantage is that only electronic-structure calculations for one  $\mathbf{k}$  point and not for pairs  $\mathbf{k}$  and  $\mathbf{k} + \mathbf{q}$  have to be performed. On the other hand, matrix elements of the complicated velocity operator instead of an exponential function have to be considered.

The relation of the dielectric function in expression (6) to the second-rank tensor  $\hat{\varepsilon}(\omega)$  indicates that we have indeed introduced the longitudinal dielectric function  $\varepsilon_l(\mathbf{q}, \omega) = \hat{\mathbf{q}} \cdot \hat{\varepsilon}(\omega) \cdot \hat{\mathbf{q}}$ , with  $\hat{\mathbf{q}} = \mathbf{q}/|\mathbf{q}|$ . The transverse dielectric function,  $\varepsilon_t(\mathbf{q}, \omega) = \mathbf{e} \cdot \hat{\varepsilon}(\omega) \cdot \mathbf{e}$ , with a unit vector  $\mathbf{e} = \mathbf{e}(\mathbf{q}) \perp \hat{\mathbf{q}}$ , is also simply related to the dielectric tensor  $\hat{\varepsilon}(\omega)$ . For cubic crystals this tensor is diagonal,  $\varepsilon_{\alpha\beta}(\omega) = \delta_{\alpha\beta} \varepsilon(\omega)$ , with equal components independent of the choice of the Cartesian coordinate system. Consequently, longitudinal and transverse dielectric function are equal in the limit of vanishing photon wave vectors.<sup>38</sup>

The appearance of the matrix elements of the velocity operator in Eq. (7) can be also interpreted as a result of another derivation of the dielectric function starting from the vector-potential description of the electromagnetic field. In this sense, the equality of expressions (3) and (6) with (7) may be interpreted to follow as a consequence of the gauge invariance of the description of optical properties. This invariance is generally valid, even beyond the independent-particle (or independent-QP) approximation, as shown by Ambegoakar and Kohn<sup>39</sup> for cubic crystals and by Del Sole and Fiorino<sup>40</sup> for less symmetric materials.

In general, nonlocal potentials are included in the independent-particle Hamiltonian  $H$ . This happens already at the DFT-LDA level, because of the use of nonlocal pseudopotentials. This fact makes the calculation of the matrix elements of the velocity operator more difficult. Since the Hamiltonian has the formal structure  $H = \mathbf{p}^2/2m + V_l + V_{nl}$ , where the total potential,  $V = V_l + V_{nl}$ , is divided into a local ( $l$ ) and a nonlocal ( $nl$ ) part and the momentum operator  $\mathbf{p}$  is introduced, the velocity operator (5) can be transformed into the representation,<sup>2</sup>

$$v_\alpha = p_\alpha/m + \frac{i}{\hbar} [V_{nl}, x_\alpha]_-, \quad (8)$$

where  $V_{nl}$  denotes the spatially nonlocal contribution to the effective total potential in the single-particle equations and  $p_\alpha$  is a Cartesian component of the momentum operator. Equation (8) indicates that a naive approximation of the electron-photon interaction, which ends up with expression (7), but with the replacement of  $v_\alpha$  by  $p_\alpha/m$ , in general, violates the gauge invariance and can be only applied in the limit of local pseudopotentials and neglecting QP effects.

When QP effects are included, the spatial nonlocality of the self-energy may be treated in the same manner as the potential  $V_{nl}$ . However, in addition, a problem arises from the energy shift  $\Delta_n(\mathbf{k})$  of the DFT-LDA eigenvalues  $\varepsilon_n^0(\mathbf{k})$  to  $\varepsilon_n(\mathbf{k})$ , the position of the main peak in the spectral function of the single-QP Green function. Within the assumption of nearly equal DFT-LDA and QP wave functions and neglecting nonlocality effects in the optical transition operator, this problem has been originally attacked by Levine and Allan<sup>5</sup> and Del Sole and Girlanda.<sup>27</sup> They applied Eq. (4) only in the form where the single-particle energies are replaced by those of the DFT-LDA,  $\varepsilon_n^0(\mathbf{k})$ , whereas the energies in expression (3) are taken as the QP ones,  $\varepsilon_n(\mathbf{k})$ . As the result formula (7) is obtained, however with an additional renormalization factor  $[\varepsilon_c(\mathbf{k}) - \varepsilon_v(\mathbf{k})]^2 / [\varepsilon_c^0(\mathbf{k}) - \varepsilon_v^0(\mathbf{k})]^2$ , which increases the oscillator strengths according to the increase of the averaged gap and, consequently, the high-frequency dielectric constant. Meanwhile, first attempts<sup>41</sup> exist to include also the consequences of dynamical screening effects in the QP self-energy. However, the resulting strong reduction of the absorption spectra indicates that these effects have to be taken into account more consistently.

### C. $f$ -sum rule

In the limit  $\eta \rightarrow +0$ , the oscillator-strength ( $f$ -) sum rule may be easily obtained, because of the appearance of the Dirac's  $\delta$  function as a consequence of the energy conservation. We restrict ourselves to the case, where the microscopic spatial inhomogeneity of the matter, i.e., the local-field effects, can be neglected. We start from the longitudinal dielectric function in expression (3), but sum up over all bands instead only the unoccupied ones. A proof of that extension can be easily given by an exchange of the occupied band states in the additional terms that have to be subtracted. One obtains

$$\begin{aligned} &\int_{-\infty}^{\infty} \frac{d\omega}{\pi} \omega \operatorname{Im} \varepsilon_l(\hat{\mathbf{q}}, \omega) \\ &= \lim_{\mathbf{q} \rightarrow 0} v(\mathbf{q}) \frac{4}{V\hbar^2} \sum_{\mathbf{k}, \mathbf{k}'} \sum_{n=c,v} \sum_v [\varepsilon_n(\mathbf{k}) - \varepsilon_v(\mathbf{k}')] \\ &\quad \times |\langle n\mathbf{k} | e^{i\mathbf{q}\mathbf{x}} | v\mathbf{k}' \rangle|^2. \end{aligned} \quad (9)$$

By means of relation (4), one of the matrix elements on the right-hand side (rhs) can be rewritten as a matrix element of the operator  $[e^{i\mathbf{q}\mathbf{x}}, H]_-$  and the sum over all Bloch states  $|n\mathbf{k}\rangle$  can be performed. On the rhs, diagonal matrix elements of the operator  $e^{-i\mathbf{q}\mathbf{x}} [e^{i\mathbf{q}\mathbf{x}}, H]_-$  with valence states occur. The limit  $\mathbf{q} \rightarrow 0$  can be calculated in a similar way as by the introduction of the velocity operator in Eq. (5) and its ex-

plicit representation in Eq. (8). Replacing the diagonal matrix element of the velocity operator by  $\nabla_{\mathbf{k}}\varepsilon_v(\mathbf{k})/\hbar$  and taking into account that  $\sum_{\mathbf{k}}\nabla_{\mathbf{k}}\varepsilon_v(\mathbf{k})=0$ , one derives

$$\int_{-\infty}^{+\infty} \frac{d\omega}{\pi} \omega \operatorname{Im}\varepsilon_f(\hat{\mathbf{q}}, \omega) = \omega_p^2 \left\{ 1 - \lim_{\mathbf{q} \rightarrow 0} \sum_{\alpha, \beta=x, y, z} \frac{q_\alpha q_\beta}{q^2} \frac{2m}{\hbar^2 \bar{n} V} \times \sum_{\mathbf{k}} \sum_v \langle v\mathbf{k} | [ [V_{nl}, x_\alpha]_-, x_\beta ]_- | v\mathbf{k} \rangle \right\}, \quad (10)$$

where the definitions of the averaged electron density  $\bar{n}=(2/V)\sum_{\mathbf{k}}\sum_v$  and the plasma frequency of the valence electrons  $\omega_p^2=4\pi e^2\bar{n}/m$  are used.

Considering expression (10), a word of caution is necessary. Taking into account nonlocal contributions to the potential in the single-particle Hamiltonian, the Thomas-Reiche-Kuhn  $f$ -sum rule is violated. This is somewhat surprising since, usually, the RPA, i.e., the approximation of the two-particle Green function as a product of two single-particle Green functions, should not give rise to a violation of the sum rule. It seems that in the presence of nonlocal potentials the representation of the two-particle excitation energies as differences of band energies is not more possible, even without taking into account electron-hole Coulomb interaction. In other words, even when excitonic effects are neglected, the total many-body Hamiltonian cannot be simply replaced by a sum of effective single-particle Hamiltonians in the presence of nonlocal pseudopotentials or QP self-energies.<sup>27</sup> Previously, other authors<sup>5,7,22,30</sup> has noted this problem. Meanwhile, it is also discussed<sup>7</sup> in the case of the Johnson  $f$ -sum rule,<sup>42,43</sup> i.e., when local fields  $\mathbf{G} \neq \mathbf{G}'$ , as in expressions (1) and (2), have been included.

The second term on the rhs of Eq. (10) represents an additional oscillator strength induced by nonlocal potentials when the total Hamiltonian is represented by a sum of effective single-particle ones. Considering this reason, the  $f$ -sum rule may be reformulated according to Levine and Allan,<sup>5</sup> by introducing the square of an “effective plasma frequency”  $(\omega_p^{\text{eff}})^2$  related to the rhs of Eq. (10). Consequently, an effective (pseudo-) valence electron density occurs that is modified with respect to the averaged density  $\bar{n}$  by the nonlocality. A physical discussion of this effect is given in Ref. 5 (cf. also references therein). It is based on the fact that in the pseudopotential construction the core electrons are removed.

### C. Numerical details

The electronic-structure calculations underlying the computations of the optical properties are based on the DFT-LDA.<sup>44</sup> The many-body electron-electron interaction is described within LDA, more precisely within the Ceperley-Alder scheme,<sup>45</sup> as parametrized by Perdew and Zunger.<sup>46</sup> The electron-ion interaction is treated by norm-conserving, *ab initio*, fully separable pseudopotentials in the KB form.<sup>29</sup> They are based on relativistic all-electron calculations for the free atoms by solving the Dirac equation self-consistently. In

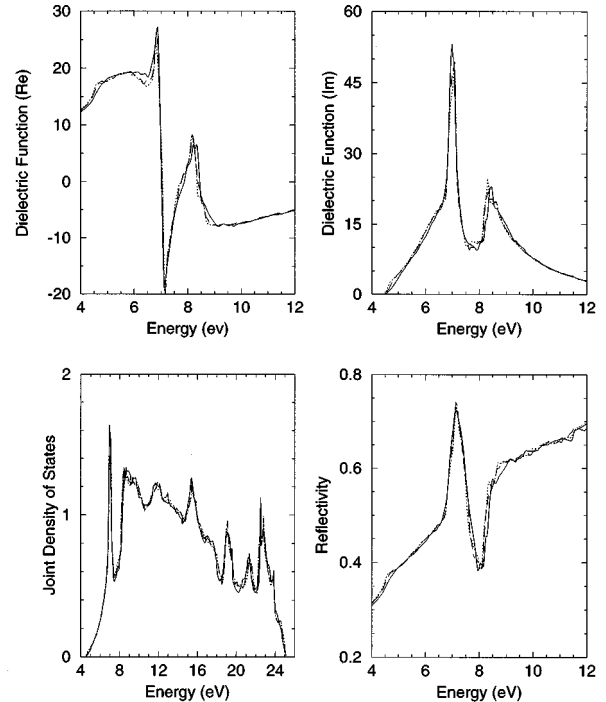


FIG. 1. Real and imaginary part of dielectric function, joint density of states, and reflectivity of SiC for different numbers  $N_{\mathbf{k}}$  of  $\mathbf{k}$  points within the irreducible part of the BZ. The velocity gauge Eq. (7) is used, but nonlocality contributions to the optical transition operator are omitted. Solid line:  $N_{\mathbf{k}}=89$ ; dashed line:  $N_{\mathbf{k}}=240$ ; dotted line:  $N_{\mathbf{k}}=505$ .  $N_{\text{CB}}=4$ .

the beginning of our studies, the pseudopotentials were generated for Si and C according to the data of Ref. 47, giving rise to potentials similar to those of BHS.<sup>28</sup> Unfortunately for this choice of the carbon pseudopotentials, too many plane waves have to be taken into account to reach convergence. Therefore, the C potentials are softened by careful choosing of the core radii.<sup>48,49</sup> The electronic wave functions are expanded in terms of plane waves. The energy cutoffs for the plane-wave expansion are chosen to 15, 34, and 42 Ry for silicon (Si), silicon carbide (SiC), and diamond (C). They are sufficient for converged energy and lattice calculations. The total-energy optimization gives rise to theoretical cubic lattice constants of  $a=10.227$  a.u. for Si,  $a=8.109$  a.u. for SiC, and  $a=6.681$  a.u. for C. They are used, although they slightly underestimate the experimental ones<sup>50</sup> and, hence, enlarge somewhat the DFT-LDA transition energies. The QP corrections to the DFT-LDA eigenvalues are computed within the  $GW$  approximation for the XC self-energy,<sup>20–25</sup> according to a simplified scheme developed by Cappellini and co-workers.<sup>51–53</sup> Using the numerical input described above, corresponding shift values have been published for zinc-blende SiC in Ref. 54. In the self-energy calculations, the number of conduction bands  $N_{\text{CB}}$  is typically restricted to a value of  $N_{\text{CB}}=60$ . In the case of the dielectric function, the sufficient number  $N_{\text{CB}}$  is tested.

The longitudinal dielectric function is calculated within both the length gauge, according to expression (3) and the velocity gauge according to Eqs. (6) and (7). First, the imaginary part  $\operatorname{Im}\varepsilon(\omega)$  is computed. The  $\mathbf{k}$ -space integration is performed numerically by means of the linear analytic tetra-

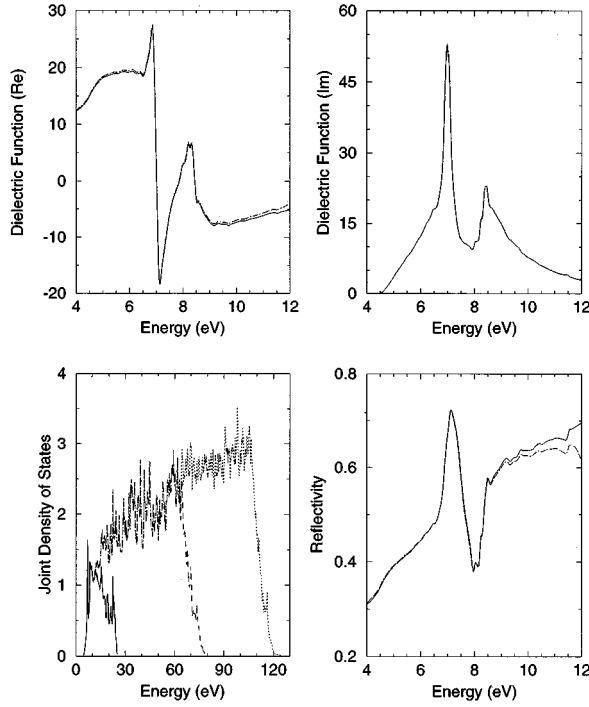


FIG. 2. The same quantities as in Fig. 1, but for different numbers  $N_{CB}$  of conduction bands. Solid line:  $N_{CB}=4$ ; dashed line:  $N_{CB}=30$ ; dotted line:  $N_{CB}=60$ .  $N_k=89$ .

hedron method,<sup>55,56</sup> usually based on 89  $\mathbf{k}$  points in the  $\frac{1}{48}$ th irreducible wedge of the Brillouin zone (BZ) of the fcc structure. However, larger numbers  $N_k$  have also been checked, as demonstrated in Fig. 1. Generally, the inclusion of more  $\mathbf{k}$  points does not produce any significant changes in the spectra. Only the peak maxima are slightly reduced and, in the high-energy case, also somewhat shifted. We use the fact that the dielectric tensor should be a scalar and compute its trace,  $\varepsilon(\omega)=[\varepsilon_{xx}(\omega)+\varepsilon_{yy}(\omega)+\varepsilon_{zz}(\omega)]/3$ , for which the restriction to the irreducible part of the BZ is valid. This corresponds to the method of invariants. The real part of the dielectric function,  $\text{Re}\varepsilon(\omega)$ , is obtained by a Kramers-Kronig transformation of  $\text{Im}\varepsilon(\omega)$ , in which a tail of the form  $(\beta\omega)/[(\hbar\omega)^2+\gamma]^2$ , as used by other authors,<sup>3,19,57</sup> is attached for energies  $\hbar\omega$  greater than  $\hbar\omega_0=17.8$  (Si), 25 (SiC), or 35 (C) eV, where  $\gamma$  is fixed to be equal to 4.5 eV. The parameter  $\beta$  is determined by the continuity of  $\text{Im}\varepsilon(\omega)$  at  $\hbar\omega_0$ . To reduce the influence of numerical fluctuations on  $\beta$ , the function  $\text{Im}\varepsilon(\omega)$  is fit in the interesting frequency region around  $\omega_0$ . Because of the large values  $\hbar\omega_0$  used, we find the tail of minor importance. In the worst case (diamond, many conduction bands), the variation of the dielectric constant  $\varepsilon_\infty$ , as well as of the plasma frequency  $\omega_p^{\text{eff}}$ , is smaller than 1%.

Another important input parameter is the number of conduction bands  $N_{CB}$  taken into account. The influence of  $N_{CB}$  is indicated in Fig. 2, in the case of cubic SiC. No noticeable differences were found for  $\text{Im}\varepsilon(\omega)$  in the energy range of interest. The same holds for  $\text{Re}\varepsilon(\omega)$  around the frequency of the most pronounced oscillator. However, its increase in the high-energy region produces a remarkable reduction of the reflectivity for these frequencies. Surpris-

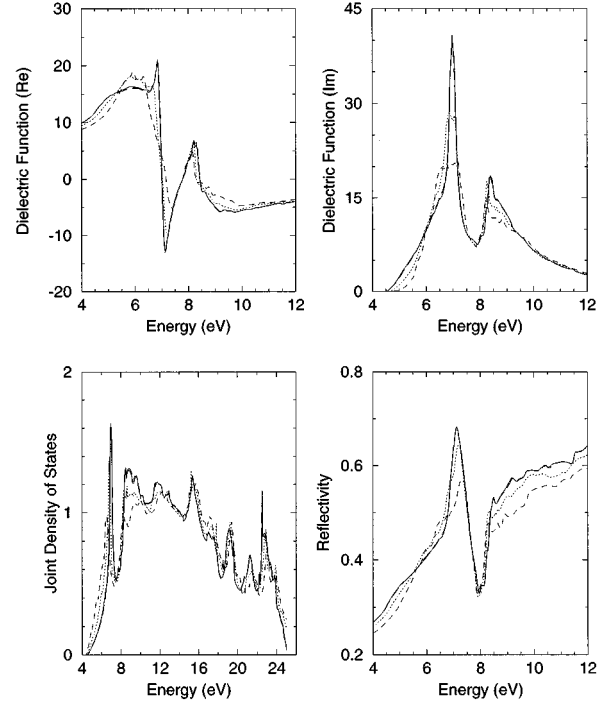


FIG. 3. Longitudinal dielectric function, Eq. (3), without local-field corrections for SiC in dependence on the wave vector with a finite component  $q = \kappa 2\pi/a$  parallel to a Cartesian axis. Solid line:  $\kappa = 1/160$ ; long-dashed line:  $\kappa = 1/80$ ; dotted line:  $\kappa = 1/16$ , dashed line:  $\kappa = 1/8$ .  $N_k=89$ ,  $N_{CB}=4$ .

ingly, in a wide energy range until the main structure in the reflectivity spectrum, four conduction bands are sufficient for optical properties. The reason are the matrix element effects that significantly reduce the influence of the joint density of states, because the transition probabilities become small for high energies.

The transition matrix elements are calculated by different methods. For zero reciprocal lattice vectors and applying the Coulomb gauge matrix elements of the type  $\langle c\mathbf{k}|e^{i\mathbf{q}\cdot\mathbf{x}}|v\mathbf{k}'\rangle$  in Eq. (3) are computed using the results of two different electronic-structure calculations at the Bloch wave vectors  $\mathbf{k}$  and  $\mathbf{k}+\mathbf{q}$ , with a certain small but finite wave vector  $\mathbf{q}$ . Usually, we have considered wave vectors with a nonvanishing Cartesian component  $q = 2\pi/a/80$ . From Fig. 3, it follows that this value is reasonable. Smaller values do not change the dielectric function. On the other hand, values large compared to the photon wave vector give rise to remarkably broadened line shapes.

In the case of the Coulomb gauge Bloch matrix elements of the velocity operator in Eq. (8) have to be considered. They are related to those taken between plane waves  $|\mathbf{K}\rangle$  and  $|\mathbf{K}'\rangle$  at wave vectors  $\mathbf{K}=\mathbf{k}+\mathbf{G}$  and  $\mathbf{K}'=\mathbf{k}+\mathbf{G}'$ . It follows<sup>2</sup>

$$\langle \mathbf{K} | \mathbf{v} | \mathbf{K}' \rangle = \frac{\hbar}{m} \mathbf{K} \delta_{\mathbf{K}\mathbf{K}'} + \frac{1}{\hbar} (\nabla_{\mathbf{K}} + \nabla_{\mathbf{K}'}) \langle \mathbf{K} | V_{\text{nl}} | \mathbf{K}' \rangle. \quad (11)$$

The fully separable pseudopotentials in the KB form<sup>29</sup> allows a factorization according to

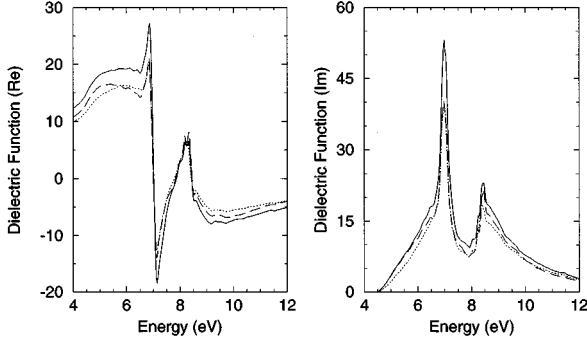


FIG. 4. Dielectric function for SiC. Solid line: velocity gauge [Eq. (7)], but neglecting the nonlocal pseudopotential contribution in the transition operator [Eq. (8)]; dashed line: full velocity gauge, including nonlocal contributions; dotted line: length gauge Eq. (3).  $N_{\mathbf{k}}=89$ ,  $N_{\text{CB}}=4$ .

$$\begin{aligned} \langle \mathbf{K} | V_{\text{nl}} | \mathbf{K}' \rangle &= \sum_s \exp[i(\mathbf{K} - \mathbf{K}') \cdot \mathbf{t}_s] \\ &\times \sum_{l=0}^1 \sum_{m=-l}^l C_l F_{lm}^s(\mathbf{K}) F_{lm}^{s*}(\mathbf{K}'), \\ F_{lm}^s(\mathbf{K}) &= \int d^3\mathbf{r} e^{-i\mathbf{K}\mathbf{r}} V_l^s(r) \Phi_{lm}^{ps}(\mathbf{r}), \end{aligned} \quad (12)$$

with the nonlocal contribution  $V_l^s(r)$  of the ionic pseudopotential localized at the point  $\mathbf{t}_s$  in the unit cell, the pseudowave function  $\Phi_{lm}^{ps}(\mathbf{r})$  of the corresponding atom, and a normalization constant  $C_l$ .<sup>58</sup>

### III. APPLICATION TO SILICON, SILICON CARBIDE, AND DIAMOND

#### A. Gauge dependence in explicit calculations

In order to study the gauge influence, the dielectric function is represented for SiC, in the framework of certain numerical approximations in Fig. 4. Silicon carbide is selected as a model substance. First, we consider the velocity gauge in Eq. (7). Generally, we find that the nonlocal pseudopotentials are of remarkable influence on the optical transition operator in Eq. (8), as well as the resulting dielectric function. In the case of the stronger bonded group-IV materials, e.g., SiC, we observe a reduction of the amplitude of the dielectric function by about 10–25 % in the average, due to the nonlocality effects. The physical reason of the reduction is not very clear. We expect a small increase of the amplitudes, since the nonlocal contributions to the pseudopotential give rise to a small gap opening. In the case of GaAs, not shown here, indeed we find such an enlargement. There seems to be an opposite tendency changing from free-electron-like materials to crystals containing first-row elements, where the wave functions are stronger localized. The polarizability is effectively reduced by the nonlocality contributions. In a local picture, this would be consistent with a spatial redistribution of the oscillator strength. In the case of materials, such as GaAs, there is an additional influence from the energetically highly lying  $d$  electrons. They have a remarkable influence in constructing the nonlocal part of the atomic pseudo-

potentials. In any case, we conclude that within the transversal gauge, the replacement of the velocity operator by the momentum operator gives rise to a certain error, depending on the bonding properties of the material considered.

The small discrepancies between the dielectric functions in length and velocity gauge in Fig. 4 are somewhat surprising, although practically they only concern the frequency regions below and above the main peaks. In general, the module of the dielectric function is overestimated by changing from the longitudinal perturbation to the transversal gauge. As a consequence, the equality of the dielectric functions in the two gauges is slightly violated for the considered cubic crystals Si, SiC, and C.

Two reasons for the discrepancies may be mentioned. First, one assumption used in the derivation of expressions (6) and (7) from Eq. (3) must be invalid, due to the applied numerical approximations. Relation (4) is only based on the validity of the Kohn-Sham equations independent of the details of the wave-function description and the diagonalization procedure. On the other hand, the explicit representation (8) of the velocity operator (5) starts from the assumption that the local part of the single-particle Hamiltonian,  $H_l = \mathbf{p}^2/2m + V_l$ , gives rise to the momentum operator when it commutes with the space operator. However, the commutator relation  $im[H_l, x_\alpha]_- = \hbar p_\alpha$  involves the orthogonality and the completeness of the eigenfunctions  $|n\mathbf{k}\rangle$ . More strictly speaking,  $x_\alpha$  and  $p_\beta$  cannot exactly obey the underlying commutator relation  $[\mathbf{x}, \mathbf{p}]_- = i\hbar \mathbf{1}$  in any finite basis set. This relation cannot hold in a representation with only a finite number of basis states, as has recently been pointed out in the case of a restricted tight-binding basis.<sup>59</sup> In our case of a plane-wave expansion, one uses a finite basis of plane waves limited by the energy cutoff. Moreover, we restrict the number  $N_{\text{CB}}$  of conduction bands, as well as the number of  $\mathbf{k}$  points  $N_{\mathbf{k}}$ , with the consequence that the closure relation  $\sum_{n,\mathbf{k}} |n\mathbf{k}\rangle \langle n\mathbf{k}| = \mathbf{1} + \Delta(N_{\text{CB}}, N_{\mathbf{k}})$  is only fulfilled with a deviation  $\Delta(N_{\text{CB}}, N_{\mathbf{k}})$ . A nonlocal function  $\Delta(N_{\text{CB}}, N_{\mathbf{k}})$  appears on the rhs, which vanishes in the limits  $N_{\text{CB}} \rightarrow \infty$  and  $N_{\mathbf{k}} \rightarrow \infty$ . In our explicit numerical calculations, this unphysical nonlocality appears and enlarges the dielectric function somewhat for the transverse gauge. Second, in principle, the calculations of the dielectric function starting from a longitudinal perturbation are converged with respect to the small wave vector. However, a small increase of the spectra changing the wave vector from  $\kappa = 1/80$  to a smaller value cannot be excluded (cf. Fig. 3).

#### B. Quasiparticle effects

The calculation of optical spectra with the inclusion of QP effects is complicated by the nonlocality and energy dependence of the self-energy. As a consequence of the latter, the spectral behavior of the single particles is different from a shifted Dirac's  $\delta$  function with the full spectral weight.<sup>60</sup> This leads to a strong (by about one third) reduction of the optical oscillator strength.<sup>41</sup> However, there are indications that dynamical vertex corrections may (at least partially) cancel such a reduction. Therefore, at present, we neglect dynamical effects, as in all calculations up to now, and briefly recall how the self-energy nonlocality can be handled.<sup>27</sup>

The presence of a nonlocal self-energy, as well as of a nonlocal pseudopotential, does not affect the linear-response formulation in the case of a longitudinal perturbation. Hence, equation (3) remains valid, with QP corrections embodied in the band energies. Also, the transformation to the transverse gauge described in Sec. II B remains valid, together with equation (7). The problem is that the matrix elements of the velocity operator (5) must be used herein, which include complicated terms arising from the nonlocality of the self-energy contained in  $H$ . In order to avoid their calculation, we exploit the aforementioned similarity of DFT-LDA and QP wave functions. We use Eq. (4), with the DFT-LDA Hamiltonian  $H^0$ : hence, the energy eigenvalues in Eq. (4) are the DFT-LDA ones. Coming to equation (7), the recipe for dealing with nonlocal self-energy effects is clear: only the single-particle energies, which arise from the spectral behavior of the single-electron as well as single-hole Green function, are replaced by the QP values,<sup>60</sup> but not those occurring due to the rewriting of optical matrix elements as argued in Sec. II B. In a naive approach, all single-particle energies appearing in expression (7) are shifted by the QP corrections. This leads, however, to the breaking down of the gauge invariance, as discussed above, and to a strong reduction of oscillator strengths. Therefore, the naive approach is incorrect, and calculations carried out according to it will be shown, in this paper, only for the sake of comparison. In order to better evidenciate the nonlocality of the self-energy, that of the pseudopotential will be neglected, namely, only the first term on the right-hand side of Eq. (11) is retained for the velocity operator.

Consequently, in the computations, only the DFT-LDA single-particle energies, which arise from the spectral behavior of Green's functions, are corrected by wave-vector- and band-index-dependent QP shifts  $\Delta_n(\mathbf{k})$ . For SiC, such values have been published in Ref. 54. For Si and C, they are calculated according to the same scheme.

The results of changing the single-particle energies in two ways from the DFT-LDA to the QP values is presented in Fig. 5 for silicon, silicon carbide, and diamond. At first sight, the main effect of the QP corrections looks like the application of a scissors operator,<sup>23,26,61</sup> with a rigid shift  $\Delta$  of the conduction bands against the valence bands averaged over combinations of QP shifts of the Bloch states. In the naive approximation, it simply holds  $\text{Im}\epsilon(\omega) = [\hbar\omega/(\hbar\omega + \Delta)]^2 \text{Im}\epsilon^{\text{DFT}}(\omega - \Delta/\hbar)$ , like in the results of Levine and Allan.<sup>5</sup> A similar rough description is possible for the real part in a wide frequency range for not too small frequencies. However, in the static case, the frequency in the prefactor has to be replaced by the average gap of the system. If only the spectral properties are changed, one finds  $\text{Im}\epsilon(\omega) = \text{Im}\epsilon^{\text{DFT}}(\omega - \Delta/\hbar)$ , which is correct within an independent-QP approximation.<sup>27</sup> Similarly, the real parts may be related to each other. Whereas, in the first (naive) approach, the peak intensity is remarkably changed, in the second case, the spectra are only nearly rigidly shifted, even if this shift seems to be larger for higher photon energies. The calculations shown in Fig. 5, with wave-vector and band-index-dependent QP shifts, are very similar to the second approach. The only difference not accounted for by a rigid shift is a very slight reduction of the main peak.

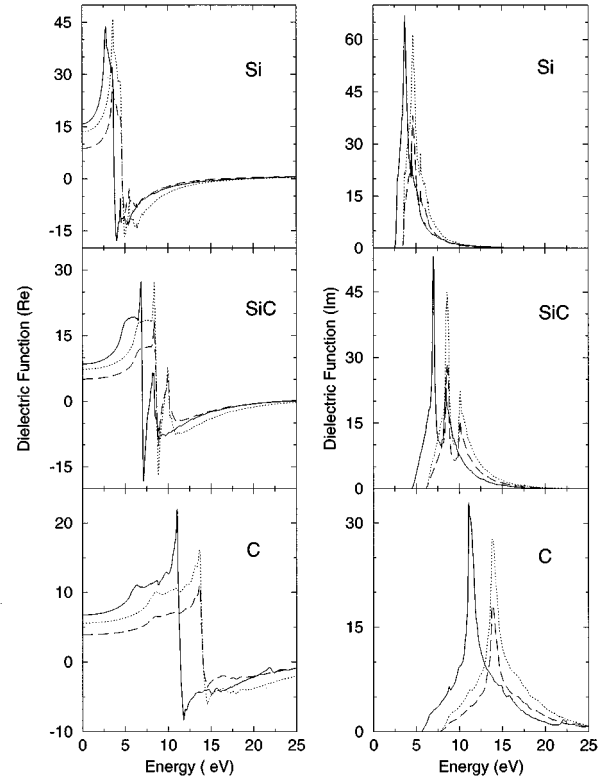


FIG. 5. Dielectric function in velocity gauge and  $v_\alpha = p_\alpha/m$ , for Si, SiC, and C. Solid line: DFT-LDA; dashed line: QP (all energies replaced); dotted line: QP (energies replaced only in single-particle Green functions).  $N_{\text{CB}}=8$  (Si, C), 4 (SiC),  $N_{\mathbf{k}}=89$ . Wave-vector- and band-index-dependent QP shifts are used.

The apparent validity of the scissors-operator approximation is somewhat surprising considering the wave-vector and band-index dependences of the QP shifts  $\Delta_n(\mathbf{k})$ . For instance, in the case of zinc-blende SiC, we have found<sup>54</sup> a remarkable variation of the shifts. The variation of  $\Delta_n(\mathbf{k})$  for the upper valence bands is as large as 0.6 eV going from the center of the BZ to its boundaries. Similar values are observed for the  $p$ -like conduction bands. The above results may be explained by two different effects acting on the dielectric function. First, the evidence of the energy shifts is modified by the curvature of the bands, i.e., the joint-density-of-states effect, and the magnitude of the corresponding matrix elements. Second,  $n$ - and  $\mathbf{k}$ -dependent QP shifts can act like rigid shifts. This is shown by Janak *et al.*<sup>62</sup> and Wang and Klein.<sup>19</sup> They started from an idea of Sham and Kohn<sup>63</sup> being valid in the case of slowly varying electron densities. According to this idea, electron-hole-pair excitation energies in DFT-LDA may be corrected by QP shifts in the form  $\Delta_c(\mathbf{k}) - \Delta_v(\mathbf{k}) = \lambda[\epsilon_c(\mathbf{k}) - \epsilon_v(\mathbf{k})]$ . It results in  $\text{Im}\epsilon(\omega) = 1/(1+\lambda) \text{Im}\epsilon^{\text{DFT}}[\omega/(1+\lambda)]$ .<sup>19</sup> With respect to the imaginary part, this result is intermediate between the two former ones. However, it takes into account that in the average, the QP effect on the excitation energies is larger for more distant bands.

In order to study the quality of a scissors-operator approximation, we have studied the influence of the wave-vector- and band-index-dependent QP shifts in Fig. 6 for the imaginary part of the dielectric function. The problem is de-

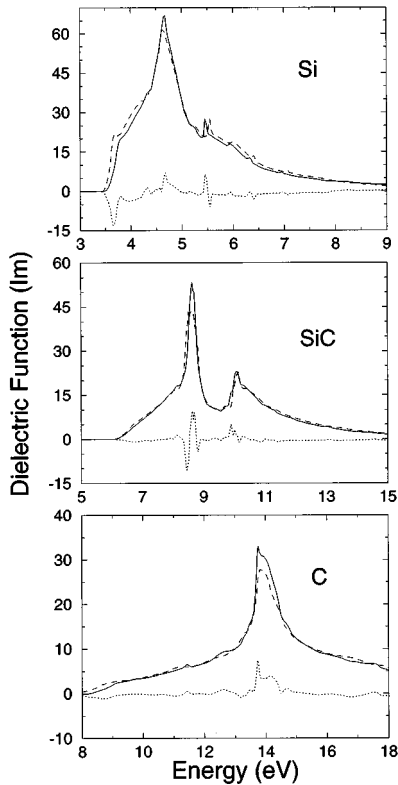


FIG. 6. Imaginary part of the dielectric function of Si, SiC, and C in QP approximation. Scissors operator: solid line; inclusion of wave-vector- and band-index-dependent QP shifts: dashed line; difference: dotted line.

fining a reasonable scissors operator  $\Delta$ . We have used the shift of the first zero in the real part of  $\varepsilon(\omega)$  from its DFT-LDA value to that within the QP approximation. The resulting values  $\Delta=0.95$  (Si), 1.65 (SiC), and 2.65 eV (C) are somewhat larger than the openings of the indirect energy gaps 0.78 (Si), 1.31 (SiC), and 1.86 eV (C), but remain below the values obtained by averaging all QP shifts. Figure 6 makes the influence of the dependence of the QP shifts on the Bloch quantum numbers  $n$  and  $\mathbf{k}$  obvious. In comparison to the simply shifted DFT-LDA spectra, one observes a tendency for broadening of the absorption spectra. The intensity of the principal peak decreases, whereas the spectral weights of the low- and high-energy tails increase. In addition, the peaks in the imaginary part are somewhat differently shifted. This holds especially for those at the high-energy side, for which the scissors operator is too small. The broadening effect is mainly due to changes in the joint density of states. The parallelism of the conduction and valence bands contributing to the principal peak is reduced by the shifts  $\Delta_n(\mathbf{k})$ , whereas other pairs of empty and occupied bands become more parallel.

### C. Sum rules

The spatial nonlocalities due to pseudopotentials and numerical uncertainties as well as the QP effects also influence the various sum rules via the spectral behavior of the underlying dielectric functions. We consider the generalized oscillator-strength sum rule [cf. Eq. (10)],

TABLE I. Dielectric constant and effective plasma frequency for three different approximations of the optical transition operator and varying number of conduction bands  $N_{\text{CB}}$  and  $\mathbf{k}$  points  $N_{\mathbf{k}}$ .  $L$ : longitudinal (length) gauge;  $T(\text{nl})$ : transverse (velocity) gauge with full velocity operator (including nonlocal contributions);  $T(I)$ : transverse gauge, where nonlocal-potential contributions are omitted.

Material	$N_{\text{CB}}/N_{\mathbf{k}}$	$\varepsilon_{\infty}$			$(\omega_p^{\text{eff}}/\omega_p)^2$		
		$L$	$T(\text{nl})$	$T(I)$	$L$	$T(\text{nl})$	$T(I)$
Si	8 / 89	13.6	14.5	15.8	0.90	1.14	1.05
	16 / 89			15.9			1.07
SiC	4 / 89	7.0	7.5	8.5	0.76	0.75	0.87
	30 / 89	7.2	7.7	8.7	0.93	0.86	1.06
	100 / 89	7.2	8.3	8.7	0.99	0.91	1.00
	4 / 240	7.1	7.6	8.6	0.72	0.76	0.87
C	4 / 505	7.4	7.6	8.6	0.75	0.75	0.87
	8 / 89	5.9	6.9	6.8	0.85	0.94	0.96
	30 / 89			6.8			0.85

$$(\omega_p^{\text{eff}})^2 = \frac{2}{\pi} \int_0^{\infty} d\omega \omega \text{Im}\varepsilon(\omega), \quad (13)$$

and the screening sum rule,

$$\varepsilon_{\infty} = 1 + \frac{2}{\pi} \int_0^{\infty} d\omega \frac{1}{\omega} \text{Im}\varepsilon(\omega), \quad (14)$$

with  $\varepsilon_{\infty} = \text{Re}\varepsilon(0)$ , which may be interpreted as a direct consequence of the Kramers-Kronig transform at zero frequency. The appearing quantities, the square of the “effective plasma frequency”  $\omega_p^{\text{eff}}$  and the (high-frequency) electronic dielectric constant  $\varepsilon_{\infty}$  represent suitable measures for the frequency-averaged effects.

The effect of the gauge of the electromagnetic field together with the incompleteness of the Bloch functions used in the numerical calculations on  $\omega_p^{\text{eff}}$  and  $\varepsilon_{\infty}$  is represented in Table I. The electronic dielectric constant  $\varepsilon_{\infty}$  reflects the same dependence on the particular gauge of the electromagnetic field as already discussed for the frequency-dependent dielectric function. In general, the largest values are observed in the transversal (velocity) gauge, neglecting the nonlocal contributions to the transition operator. The smallest ones appear in the longitudinal (length) gauge. All calculated values are larger than the experimental ones  $\varepsilon_{\infty}=11.7$  (Si), 6.7 (SiC), and 5.7 (C),<sup>50</sup> expressing the underestimation of the transition energies within the DFT-LDA. This is in agreement with the findings of other authors. With the improvement of the completeness of the eigenfunctions, i.e., increasing number of conduction bands and mesh points in  $\mathbf{k}$  space, the values of  $\varepsilon_{\infty}$  decrease. The SiC results for increasing  $N_{\mathbf{k}}$  strongly indicate the tendency for convergence of the two different gauges when the nonlocal-pseudopotential effects are not neglected and the wave functions are complete.

The total oscillator strength, represented in Table I by the square of the effective plasma frequency  $\omega_p^{\text{eff}}$  in units of the plasma frequency  $\omega_p$ , is almost smaller than 1, reflecting the reduction of the oscillator strength, due to the influence of the nonlocal potentials, as can be seen from Eq. (10). Only

TABLE II. Dielectric constant and effective plasma frequency for three different ways of inclusion of QP shifts. DFT: neglect; QP (spec): only in spectral behavior; QP (all): shift of all DFT-LDA single-particle energies. The velocity gauge (7) is used, but nonlocal effects are omitted in the transition operator.  $N_{\text{CB}}=8$  (Si, C),  $N_{\text{CB}}=4$  (SiC),  $N_{\mathbf{k}}=89$ .

Material	$\epsilon_{\infty}$			$(\omega_p^{\text{eff}}/\omega_p)^2$		
	DFT	QP (spec)	QP (all)	DFT	QP (spec)	QP (all)
Si	15.8	13.5	8.7	1.05	1.25	0.79
SiC	8.5	7.3	5.1	0.87	1.09	0.72
C	6.8	5.6	3.9	0.96	1.04	0.59

silicon exhibits larger values within the transversal gauge, indicating the more delocalized character of the wave functions as for the C-based materials (cf. above discussion). In contrast to the case of the spectral behavior, the number of BZ integration points plays no important role. After the frequency integration according to Eq. (11), the integrand represents a smooth function in  $\mathbf{k}$ . More important is the increase of the number  $N_{\text{CB}}$  of the conduction bands. In the longitudinal case, one clearly sees that  $(\omega_p^{\text{eff}}/\omega_p)^2$  approaches the value 1. We speculate that the nonlocalities, due to the incompleteness, partially compensate those related to the pseudopotentials.

The dielectric constant, as well as the oscillator strength, reacts sensitively to the QP effects (cf. Table II). The increase of the energy gaps only in the spectral behavior gives rise to smaller dielectric constants and an enlargement of the total oscillator strength roughly by a factor  $(1 + \Delta/\hbar\omega_p)^2$ . When all DFT-LDA energies are replaced by the QP values,

a remarkable reduction of  $\epsilon_{\infty}$  and  $(\omega_p^{\text{eff}}/\omega_p)^2$  happens, since the renormalization  $\sim(\hbar\omega)^2/(\hbar\omega + \Delta)^2$  of the oscillator strengths disappears. The resulting extreme reduction of both quantities confirms that the underlying approximation is rather unrealistic.

#### D. Comparison with experiment

In Fig. 7, the dielectric functions of Si, SiC, and C are calculated within the reduced velocity gauge  $v_{\alpha}=p_{\alpha}/m$  and DFT-LDA and are compared with experimental data.<sup>64–66</sup> The theoretical spectra are shifted towards higher energies by  $\Delta=0.47$  eV (Si),  $\Delta=0.84$  eV (SiC), and  $\Delta=0.40$  eV (C), to bring the zeros of the experimental and theoretical real part together. These shifts are much smaller than the state-independent opening of the energy gaps used generally<sup>68</sup> or derived from our QP calculations, especially for diamond. One reason for this finding should be excitonic effects that are not included in our calculations. The Coulomb attraction between electrons and holes gives rise to smaller transition energies. Another reason concerns the details of the underlying DFT-LDA calculations. Although the calculations are rather converged and only small reductions of transition energies with a further increase of the plane-wave cutoffs are expected, there remains an influence. We use the theoretical lattice constants in the electronic-structure calculations. They are smaller by about 1% than the experimental ones. An increase of the lattice constant, however, enlarges the transition energies. Nevertheless, the resulting theoretical spectral behavior reproduces the overall frequency dependences found experimentally. On the other hand, we have to mention that similarly small scissors operators have been found to bring the calculation of  $\epsilon_{\infty}$  in agreement with experiment.<sup>5,10</sup>

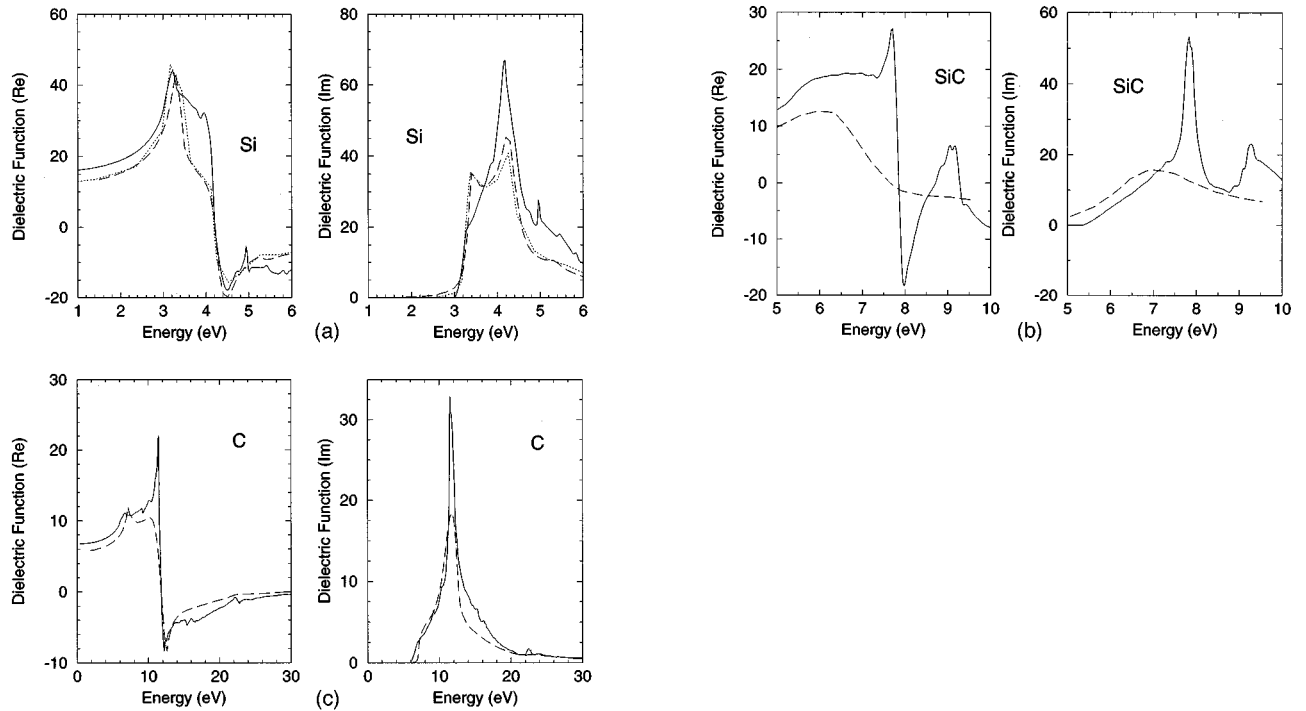


FIG. 7. Calculated dielectric functions in comparison with experimental data for Si (Refs. 64 and 65) (a), SiC (Ref. 66) (b), and diamond (Ref. 67) (c). The theoretical curves (solid lines) are taken within the reduced velocity gauge  $v_{\alpha}=p_{\alpha}/m$  and rigidly shifted by  $\Delta=0.46$  (0.84, 0.37) eV to higher energies for Si (SiC, C). Experimental data: dashed lines (Refs. 64, 66, and 67) and dotted line Ref. 65.

As a general feature of all theoretical spectra of the covalent materials Si and C, the intensity of the  $E_2$  peak,<sup>69</sup> i.e., high-energy peak in  $\text{Im}\epsilon(\omega)$ , is overestimated and more sharply peaked than observed. The reason is that  $\text{Im}\epsilon(\omega)$  is calculated without inclusion of lifetime broadening effects. Also, the surface preparation of the samples used in the measurements may influence the peak heights. Wang and Klein<sup>19</sup> have taken an empirical lifetime broadening into account to adjust the  $E_2$  peak intensity. However, such a procedure gives rise to a further reduction of the  $E_1$  peak. The  $E_1$  peak at the low-energy side of the  $\text{Im}\epsilon(\omega)$  spectra is underestimated in the Si case and appears as a shoulder. In our opinion, this underestimate may be traced back to excitonic effects. The Coulomb attraction between electron and hole drastically enhances the oscillator strength, in particular in the  $E_1$  region.<sup>18,32</sup> On the other hand, local-field effects would further reduce the intensity, leading to a poorer agreement with the experiment in this energy range.<sup>17,18,32</sup> In the wide-band-gap material C, the  $E_1$  peak seems to be rather depressed in any case. This is due to the band structure. The highest valence band and the lowest conduction band are not more parallel along the [111] direction. Hence, the corresponding pronounced peak in the joint density of states is missing.

In the case of SiC, the character of the double-peak structure in  $\text{Im}\epsilon(\omega)$  is quite different. The  $E_2$  peak related to  $X_{5v} \rightarrow X_{1c}$  transitions in the band structure is only responsible for the low-energy tail in  $\text{Im}\epsilon(\omega)$ . The low-energy peak should have  $E_0$  and  $E_1$  character and may be traced back to transitions  $\Gamma_{15v} \rightarrow \Gamma_{1c}$  and  $L_{3v} \rightarrow L_{1c}$ . However, there are also contributions from the  $\Sigma$  line. The high-energy peak, that is somewhat lower in intensity, possesses  $E'_1$ ,  $E'_0$ , and  $E_2 + \delta$  character. Contributions are related to the transitions  $L_{3v} \rightarrow L_{3c}$ ,  $\Gamma_{15v} \rightarrow \Gamma_{15c}$ , and  $X_{5v} \rightarrow X_{3c}$ . More roughly, the first peak is mainly related to transitions from the highest valence band to the lowest conduction band, whereas the high-energy peak is essentially due to transition from the highest valence band to the second conduction band. Transitions from the second highest valence band to the lowest conduction band give more or less rise to the intensity between the two peaks in  $\text{Im}\epsilon(\omega)$ . Our interpretation is in rather good agreement with a former Hartree-Fock-Slater calculation,<sup>70</sup> but slightly different from that derived within an empirical pseudopotential study.<sup>71</sup>

The comparison of the calculated spectra with experimental results<sup>64–67</sup> indicates different degrees of agreement. In the case of  $\text{Im}\epsilon(\omega)$  for diamond, the spectra approach each other. Considering the neglect of lifetime, excitonic as well as local-field effects, the agreement remains satisfying in the case of Si, although the  $E_1$  peak cannot be reproduced and the transition strengths are overestimated for higher energies. For SiC, the agreement is much poorer. The double-peak structure is smeared out in the experimental curves.

The general spectral behavior of  $\text{Re}\epsilon(\omega)$  can be reproduced by the calculations as represented in Fig. 7. In particular, this holds for diamond. In the case of silicon, the peak slightly below the  $E_1$  peak agrees well, although it is somewhat shifted to smaller energies. On the other hand, the oscillator character of the spectra below the zero transition is remarkably overestimated in the theoretical spectra. The same holds for the high-energy tails. The smearing out of the

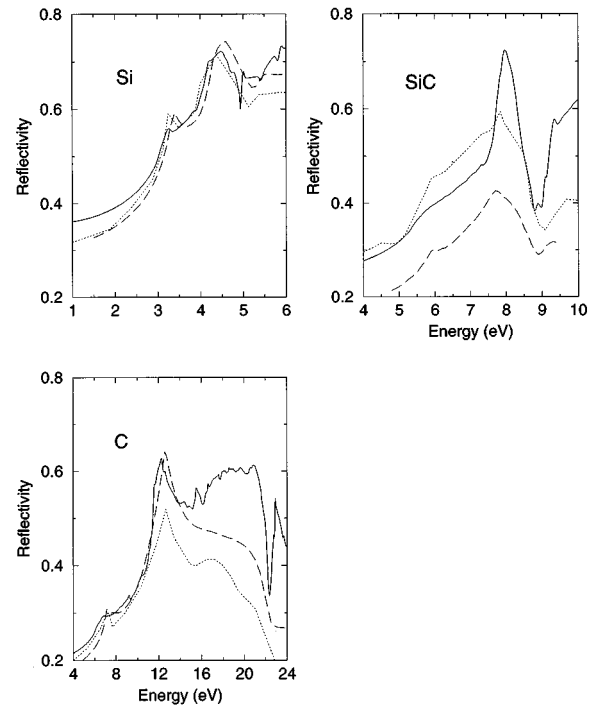


FIG. 8. Comparison of theoretical reflectivity curves (reduced velocity gauge; solid lines) with measured ones for Si [dashed line (Ref. 64), dotted line (Ref. 65)], SiC [dashed line (Ref. 73), dotted line (Ref. 72)], and C [dashed line (Ref. 68), dotted line (Ref. 74)]. The theoretical curves are rigidly shifted to higher photon energies by  $\Delta = 0.46$  eV (Si),  $\Delta = 0.84$  eV (SiC), and  $\Delta = 0.37$  eV (C).

oscillator character is most pronounced for SiC. We cannot exclude that this pronounced effect is a consequence of poor optical quality of the Bridgman crystals used in the measurements.<sup>66</sup> The consequences will be discussed in the case of the reflectivity.

Figure 8 represents a comparison of experimental and theoretical data for the reflectivity of Si, SiC, and C in a wide energy range. The theoretical curves obtained within the reduced velocity gauge and DFT-LDA have been shifted upwards by 0.46 eV (Si), 0.84 eV (SiC), and 0.37 eV (C). The experimental data are taken from Refs. 64, 65, 67, 72, 73, and 74. There is very good agreement at the low-energy side of the main peak between theory and reflectivity measurements. The only exception concerns the comparison with Ref. 73. The reflectivity of the homoepitaxial SiC layers is remarkably smaller than expected from theory and older measurements.<sup>72</sup> The reflectivity of SiC was also calculated by Lambrecht *et al.*<sup>73</sup> In order to account for variations in the sample size and the surface treatments of the samples as well as numerical uncertainties, they adjusted the low-frequency reflectivity besides the principal oscillator frequency in the real part of the dielectric function. In more detail, a multiplicative correction is applied to the interpolated experimental curves, so as to agree with the theoretical low-frequency limit  $R(4 \text{ eV}) = \frac{(n-1)^2}{(n+1)^2}$ , using the calculated value  $n = \sqrt{\text{Re}\epsilon(4 \text{ eV})}$ .

Stronger deviations between theoretical and experimental reflectivity spectra appear in the high-energy regions, in particular, for SiC and C. The theory remarkably overestimates the measurements above 9 (14) eV for SiC (C). One reason

could be that no instrumental or lifetime broadening effects are included in the theory. The disagreement above the main peak may be also explained as an artifact of the theoretical treatment. Due to the neglect of local-field effects, the dielectric function is somewhat overestimated in this frequency region. As a consequence, the reflectivity is overestimated.

#### IV. SUMMARY

We have studied the influence of two different gauges (length and Coulomb gauge) on the optical properties of group-IV materials. For vanishing photon wave vectors, the equality of the two resulting dielectric functions may be analytically demonstrated if the nonlocal contributions to the single-particle potential are fully taken into account in the optical transition operator. In the case of usually converged calculations, the agreement of the spectra is however not complete. The reason is the incompleteness of the eigenfunctions used in the explicit computations. Only when the number of mesh points in the Brillouin-zone integration and the number of conduction bands are remarkably increased, the dielectric functions with longitudinal or transversal transition operator approach each other. The artificial nonlocality due to the violation of the closure relation vanishes. However, the nonlocal contributions to the generalized velocity operator remain important.

Wave-vector and band-index-dependent quasiparticle corrections to the DFT-LDA band energies are considered in the calculation of optical properties. In the case of the dielectric function in transverse gauge, only single-particle energies appearing in the  $\delta$  function of  $\text{Im}\epsilon(\omega)$ , have to be shifted. Nevertheless, much more theoretical work has to be done to study how the frequency-dependent exchange-correlation

self-energy influences the dielectric function beyond the inclusion of these effects within DFT-LDA.

The results for the dielectric function as well as the reflectivity have been compared with experimental data. Considering the neglect of lifetime, excitonic, and local-field effects the agreement is satisfying. The variations between the functions in the various gauges are smaller than the averaged discrepancies to the experimental curves. So the particular choice seems to be unimportant. On the other hand, considering the fulfillment of oscillator-strength and screening sum rules, the results within the longitudinal-perturbation treatment may be used already for a lower number of  $\mathbf{k}$  points and bands. Shifts of the DFT-LDA eigenvalues towards higher transition energies bring the experimental and theoretical peak positions in close agreement. However, these shifts are smaller than those estimated from the quasiparticle calculations. A scissors-operator approximation is too crude.

The theory should be also improved to better describe the peak intensities and spectral distributions. Further work, concerning the *ab initio* inclusion of local-field effects due to the atomic structure of matter, of dynamical self-energy effects, as well as of the electron-hole interaction is necessary. One has to take care for the interplay of vertex variations due to dynamical screening and the dynamics in the self-energy.

#### ACKNOWLEDGMENTS

We thank P. Vogl for useful discussions and comments on the manuscript. We are indebted to P. Käckell, K. Karch, W. Windl, W.G. Schmidt, and B. Wenzien for their help with several computer codes. This work was financially supported by the Deutsche Forschungsgemeinschaft (SFB 196, Project Nos. A08 and B07) and the EC Programme Human Capital and Mobility (Contract No. ERBCHRXCT 930337).

- 
- <sup>1</sup>S. Baroni and R. Resta, Phys. Rev. B **33**, 7017 (1986).  
<sup>2</sup>M.S. Hybertsen and S.G. Louie, Phys. Rev. B **35**, 5585 (1987).  
<sup>3</sup>M. Alouani, L. Brey, and N.E. Christensen, Phys. Rev. B **37**, 1167 (1988).  
<sup>4</sup>G. de Gironcoli, S. Baroni, and R. Resta, Phys. Rev. Lett. **62**, 2853 (1989).  
<sup>5</sup>Z.H. Levine and D.C. Allan, Phys. Rev. Lett. **63**, 1719 (1989); Phys. Rev. B **43**, 4187 (1991); **42**, 3567 (1990); **44**, 12 781 (1991).  
<sup>6</sup>W.R.L. Lambrecht and B. Segall, Phys. Rev. B **40**, 7793 (1989).  
<sup>7</sup>B. Engel and F. Farid, Phys. Rev. B **46**, 15 812 (1992).  
<sup>8</sup>M.-Z. Huang and W.Y. Ching, Phys. Rev. B **47**, 9443 (1993).  
<sup>9</sup>K.-H. Lee, C.H. Park, B.-H. Cheong, and K.J. Chang, Solid State Commun. **92**, 869 (1994).  
<sup>10</sup>J. Chen, Z.H. Levine, and J.W. Wilkins, Phys. Rev. B **50**, 11 514 (1994).  
<sup>11</sup>H. Ehrenreich and M.H. Cohen, Phys. Rev. **155**, 786 (1959).  
<sup>12</sup>S.L. Adler, Phys. Rev. **126**, 413 (1962).  
<sup>13</sup>N. Wiser, Phys. Rev. **129**, 62 (1963).  
<sup>14</sup>P. Hohenberg and W. Kohn, Phys. Rev. **136**, B864 (1964).  
<sup>15</sup>W. Kohn and L.J. Sham, Phys. Rev. **140**, A1133 (1965).  
<sup>16</sup>J.P. Walter and M.L. Cohen, Phys. Rev. B **2**, 1821 (1970).  
<sup>17</sup>S.G. Louie, J.R. Chelikowsky, and M.L. Cohen, Phys. Rev. Lett. **34**, 155 (1975).  
<sup>18</sup>W. Hanke and L.J. Sham, Phys. Rev. B **21**, 4656 (1980).  
<sup>19</sup>C.S. Wang and B.M. Klein, Phys. Rev. B **24**, 3417 (1981).  
<sup>20</sup>W.E. Pickett, Comments Solid State Phys. **12**, 57 (1985).  
<sup>21</sup>F. Bechstedt, Adv. Solid State Phys. **32**, 161 (1992).  
<sup>22</sup>M.S. Hybertsen and S.G. Louie, Phys. Rev. B **34**, 5390 (1986).  
<sup>23</sup>R.W. Godby, M. Schlüter, and L.J. Sham, Phys. Rev. B **37**, 10 159 (1988).  
<sup>24</sup>L. Hedin, Phys. Rev. **139**, A796 (1965).  
<sup>25</sup>L. Hedin and S. Lundqvist, in *Solid State Physics: Advances in Research and Applications*, edited by H. Ehrenreich, F. Seitz, and D. Turnbull (Academic, New York, 1969), Vol. 23, p. 1.  
<sup>26</sup>G.A. Baraff and M. Schlüter, Phys. Rev. B **30**, 3460 (1984).  
<sup>27</sup>R. Del Sole and R. Girlanda, Phys. Rev. B **48**, 11 789 (1993).  
<sup>28</sup>G.B. Bachelet, D.R. Hamann, and M. Schlüter, Phys. Rev. B **26**, 4199 (1982).  
<sup>29</sup>L. Kleinman and D.M. Bylander, Phys. Rev. Lett. **48**, 1425 (1982).  
<sup>30</sup>A.F. Starace, Phys. Rev. A **3**, 1242 (1971).  
<sup>31</sup>E. Piparo and R. Girlanda, Nuovo Cimento D **14**, 679 (1992).  
<sup>32</sup>W. Hanke, Adv. Phys. **27**, 287 (1978).  
<sup>33</sup>J.D. Jackson, *Classical Electrodynamics*, 2nd ed. (Wiley, New York, 1975).  
<sup>34</sup>G.D. Mahan, *Many-Particle Physics*, 2nd ed. (Plenum Press, New York, 1990).

- <sup>35</sup>A. Zangwill and P. Soven, *Phys. Rev. A* **21**, 1561 (1980).
- <sup>36</sup>J. Hubbard, *Proc. R. Soc. London Ser. A* **243**, 336 (1957).
- <sup>37</sup>When QP effects are included, the eigenvalues have to be correspondingly shifted and  $H$  has to be interpreted to contain the self-energy effects in an appropriate manner.
- <sup>38</sup>H. Ehrenreich, in *The Optical Properties of Solids*, Proceedings of the International School of Physics "Enrico Fermi," edited by J. Tauc (Academic Press, New York, 1966).
- <sup>39</sup>V. Ambegoakar and W. Kohn, *Phys. Rev.* **117**, 423 (1960).
- <sup>40</sup>R. Del Sole and E. Fiorino, *Phys. Rev. B* **29**, 4631 (1984).
- <sup>41</sup>R. Del Sole and R. Girlanda (unpublished).
- <sup>42</sup>D.L. Johnson, *Phys. Rev. B* **9**, 4475 (1974).
- <sup>43</sup>M. Taut, *J. Phys. C* **18**, 2677 (1985).
- <sup>44</sup>R. Stumpf and M. Scheffler, *Comput. Phys. Commun.* **79**, 447 (1994).
- <sup>45</sup>D.M. Ceperley and B.I. Alder, *Phys. Rev. Lett.* **45**, 566 (1980).
- <sup>46</sup>P. Perdew and A. Zunger, *Phys. Rev. B* **23**, 5048 (1981).
- <sup>47</sup>R. Stumpf, X. Gonze, and M. Scheffler (unpublished); X. Gonze, R. Stumpf, and M. Scheffler (unpublished); *Phys. Rev. B* **44**, 8503 (1991).
- <sup>48</sup>B. Wenzien, P. Käckell, and F. Bechstedt, *Surf. Sci.* **307-309**, 989 (1994).
- <sup>49</sup>P. Käckell, B. Wenzien, and F. Bechstedt, *Phys. Rev. B* **50**, 17 037 (1994).
- <sup>50</sup>*Physics of Group IV Elements and III-V Compounds*, edited by O. Madelung, Landolt-Börnstein, New Series, Group III, Vol. 17, Pt. a (Springer, Berlin, 1982).
- <sup>51</sup>F. Bechstedt, R. Del Sole, G. Cappellini, and L. Reining, *Solid State Commun.* **84**, 765 (1992).
- <sup>52</sup>G. Cappellini, R. Del Sole, L. Reining, and F. Bechstedt, *Phys. Rev. B* **47**, 9892 (1993).
- <sup>53</sup>B. Wenzien, G. Cappellini, and F. Bechstedt, *Phys. Rev. B* **51**, 14 701 (1995).
- <sup>54</sup>B. Wenzien, P. Käckell, F. Bechstedt, and G. Cappellini, *Phys. Rev. B* **52**, 10 897 (1995).
- <sup>55</sup>D. Jepsen and O.K. Anderson, *Solid State Commun.* **9**, 1763 (1971); G. Lehmann and M. Taut, *Phys. Status Solidi* **54**, 469 (1972).
- <sup>56</sup>W. Windl, Diploma thesis, Universität Regensburg, 1993.
- <sup>57</sup>Y. Petroff, M. Balkanski, J.P. Walter, and M.L. Cohen, *Solid State Commun.* **7**, 459 (1968).
- <sup>58</sup>W.E. Pickett, *Comput. Phys. Rep.* **9**, 115 (1989).
- <sup>59</sup>M. Graf and P. Vogl, *Phys. Rev. B* **51**, 4950 (1995).
- <sup>60</sup>F. Bechstedt, M. Fiedler, C. Kress, and R. Del Sole, *Phys. Rev. B* **49**, 7357 (1994).
- <sup>61</sup>F. Gygi and A. Baldereschi, *Phys. Rev. Lett.* **62**, 2160 (1989).
- <sup>62</sup>J.F. Janak, A.R. Williams, and V. Moruzzi, *Phys. Rev. B* **11**, 1522 (1975).
- <sup>63</sup>L.J. Sham and W. Kohn, *Phys. Rev.* **145**, 561 (1966).
- <sup>64</sup>H.R. Philipp and H. Ehrenreich, *Phys. Rev.* **129**, 1550 (1963).
- <sup>65</sup>P.E. Aspnes and A.A. Studna, *Phys. Rev. B* **27**, 985 (1983).
- <sup>66</sup>S. Logothetidis, H.M. Polatoglou, J. Petalas, D. Fuchs, and R.L. Johnson, *Physica B* **185**, 389 (1993).
- <sup>67</sup>A.D. Papadopoulos and E. Anastassakis, *Phys. Rev. B* **43**, 5090 (1991).
- <sup>68</sup>F. Bechstedt and R. Del Sole, *Phys. Rev. B* **38**, 7710 (1988).
- <sup>69</sup>cf. nomenclature, e.g., M. Cardona, *Modulation Spectroscopy* (Academic Press, New York, 1969).
- <sup>70</sup>A.R. Lubinsky, D.E. Ellis, and G.S. Painter, *Phys. Rev. B* **11**, 1537 (1975).
- <sup>71</sup>L.A. Hemstreet and C.Y. Fong, in *Silicon Carbide—1973*, edited by R.C. Marshall, J.W. Faust, and C.Y. Ryan (University of South Carolina Press, Columbia, SC, 1974), p. 284.
- <sup>72</sup>B.E. Wheeler, *Solid State Commun.* **4**, 173 (1966).
- <sup>73</sup>W.R. Lambrecht, B. Segall, M. Yoganathan, W. Suttrop, R.P. Devaty, W.J. Choyke, J.A. Edmond, J.A. Powell, and M. Alouani, *Phys. Rev. B* **50**, 10 722 (1994).
- <sup>74</sup>W.C. Walker and J. Osantovski, *Phys. Rev.* **134**, A153 (1964).